Chapter 5

Microwave Power Transmission Based on Retro-reflective Beamforming

Xin Wang and Mingyu Lu

Additional information is available at the end of the chapter

http://dx.doi.org/10.5772/62855

Abstract

Microwave power transmission has the potential to supply wireless power to portable/mobile electronic devices over long distances (on the order of meters or even kilometers) efficiently. Nevertheless, several technical challenges remain to be resolved in order to accomplish practical microwave power transmission systems, including (i) minimizing power loss due to microwave propagation, (ii) preventing humans and other electrical systems from exposure to excessive microwave radiation, and (iii) reconfiguring wireless power transmission in reaction to environmental changes (such as physical movements of portable devices) in real time. In this chapter, a microwave power transmission scheme based on retro-reflective beamforming is proposed to address the above challenges. In the retro-reflective beamforming, wireless power transmission is guided by pilot signals. To be specific, one or more than one mobile device(s) broadcast pilot signals to their surroundings, and based on analyzing the pilot signals, a wireless power transmitter delivers focused power beam(s) onto the mobile device(s). Preliminary numerical and experimental results are presented to demonstrate the feasibility of the proposed retro-reflective beamforming scheme.

Keywords: microwave power transmission, antenna array, retro-reflective beamforming, pilot signals, microwave power focusing

1. Introduction

Microwave power transmission has been actively pursued for more than 50 years as one of the possible technologies to deliver electrical power wirelessly [1–3]. The microwave power transmission technique employs propagating electromagnetic waves in the microwave frequency range as the carrier of wireless power. Compared with techniques based on induc-

tive coupling [4], microwave power transmission has the potential to reach longer distances (on the order of meters or even kilometers). Meanwhile, microwave power transmission enjoys several advantages relative to optical power transmission [5]. First, microwave has better penetration compatibility than optical waves. Second, the conversion efficiency between DC power and microwave power is usually higher than that between DC power and optical power. Third, microwave beams can be steered straightforwardly through the phase control, whereas beam steering without resorting to mechanical motion is much more difficult in the optical regime. In 1960s, Brown [6] successfully demonstrated supplying microwave power from a ground station to a helicopter, which is probably the first impactful demonstration of microwave power transmission in the history. Since 1970s, a range of research efforts are conducted on using microwave beam to deliver power from satellites to the earth, albeit to date its feasibility is still under evaluation [7]. A case study from 1997 to 2004 is reported in the studies of Lan Sun Luk [8] and Celeste et al. [9] to construct a point-to-point wireless electricity transmission to a small isolated village called Grand-Bassin in France. An antenna array was developed by the University of Colorado in 2008 to harvest 100 mW power from a transmitter 1 meter away [10]. In 2009, the feasibility of using a car-borne power broadcaster to power sensors installed over a bridge is studied in the work of Mascarenas et al. [11]. Today, many researchers are investigating taking advantage of microwave power transmission to eliminate/relieve the battery life bottleneck of mobile/portable electronic devices [12]. Despite of its long research history, several technical challenges remain to be resolved before microwave power transmission can be applied in practice, as elaborated below.

(i) Efficiency improvement

In microwave power transmission, power loss is mainly attributed to two factors: microwave-to-DC conversion and microwave propagation. With the development of novel rectennas, the microwave-to-DC conversion loss has been reduced to less than 20% [13, 14]. In order to improve the microwave propagation efficiency, beamforming (i.e., focusing electromagnetic fields in space) is the only effective means. Beamforming can be achieved straightforwardly using highly directive antennas when both the wireless power transmitter and wireless power receiver are stationary [8]; however, it is challenging when multiple mobile/portable devices residing in a large region need wireless power simultaneously. Traditional phased-array beamforming [15] does not constitute an ideal solution, since it fails when the line-of-sight path between the phased array and the target receiver is blocked by obstacles.

(ii) Safety assurance

Excessive microwave radiation may produce hazardous effects to human bodies as well as electrical devices. Thus, while wireless power is transmitted to target receivers, it is vital to ensure that humans and other electrical systems in the surroundings are not under intensive microwave illumination. As a matter of fact, a range of regulations have been established by various agencies for microwave radiation to safeguard human safety and electromagnetic compatibility [16–18].

(iii) Real-time reconfigurability

A practical microwave power transmission system must be capable of reconfiguring itself in reaction to the environmental changes (such as physical movements of portable devices) in real time, to maintain high efficiency and safety performance.

In order to address the above challenges, a retro-reflective beamforming scheme is proposed in this chapter. In the proposed scheme, one or more than one wireless power receiver(s) broadcast *pilot signals*, a wireless power transmitter receives the pilot signals, and based on analyzing the pilot signals, the wireless power transmitter constructs focused microwave beam(s) to deliver wireless power to the receiver(s). In other words, before transmitting wireless power, the wireless power transmitter plays the role of radar: it tracks the locations of mobile/portable receivers through analyzing pilot signals broadcasted by the receivers. Based on the outcome of radar tracking, the wireless power transmitter constructs spatially dedicated channels to deliver wireless power to the receivers, which minimizes the power loss associated with microwave propagation. As a radar, the wireless power transmitter is able to identify obstacles along the line-of-sight path toward the wireless power receivers such that it could avoid directly illuminating power beams onto humans or other objects. The proposed scheme is highly reconfigurable because wireless power transmission is guided by pilot signals. Specifically, wireless power is always focused onto the locations from which pilot signals stem. As a result, as long as the target receivers broadcast pilot signals periodically, wireless power beams would follow their motions dynamically. A range of numerical and experimental studies have been conducted to verify the feasibility of the proposed retro-reflective beamforming scheme [19–21]. The numerical and experimental results demonstrate that the proposed retro-reflective beamforming scheme is able to track mobile receivers' locations and focus wireless power onto the receivers' locations in real time.

2. Retro-reflective beamforming scheme and numerical modeling

The proposed retro-reflective beamforming scheme is illustrated in a typical indoor environment shown in **Figure 1**. The wireless power transmitter consists of a base station and multiple charging panels. The charging panels are mounted over the ceiling or walls. Each charging panel includes an array of planar antenna elements. The base station and charging panels are connected through cables. Mobile/portable devices in the room receive wireless power from the wireless power transmitter through the following two steps.

Step (1) One or more than one device(s) broadcast pilot signals.

Step (2) In response to the pilot signals, the charging panels jointly construct focused (that is, dedicated) microwave power beam(s) onto the target device(s).

When the mobile/portable devices are in motion, the microwave power beams would follow the devices' locations dynamically as long as the devices broadcast pilot signals periodically. A charging panel transmits power only if it has line-of-sight interaction with the target

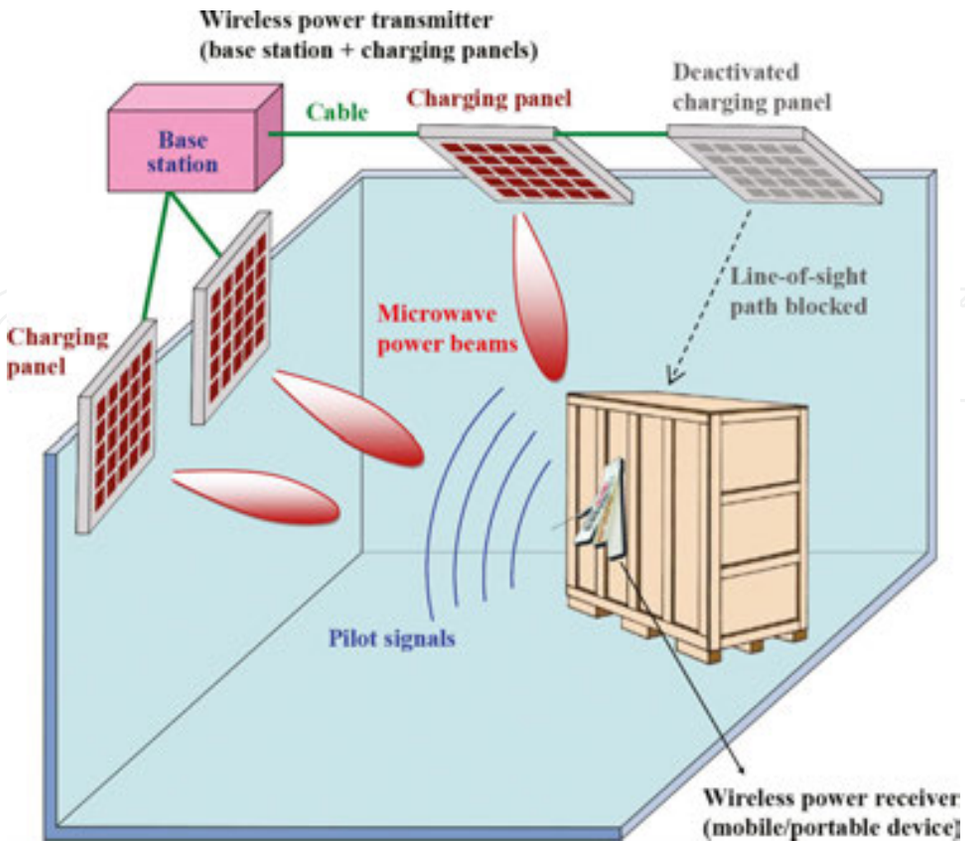

Figure 1. Depiction of wireless power transmission based on retro-reflective beamforming.

device(s); if the line-of-sight path is blocked by any obstacle, the charging panel is deactivated such that the obstacle, which might be human being, is not illuminated by power beams directly.

The underlying theory of retro-reflective beamforming is "time-reversal," which takes advantage of channel reciprocity to accomplish a space-time matched filter [22]. Specifically, propagation of pilot signals follows the "channel from target devices to charging panels," whereas propagation of microwave power beams follows the "channel from charging panels to target devices." If these two channels are reciprocal to each other and if the microwave power transmission is tailored to be the retro-reflected version of pilot signals, microwave power is spatially focused onto the locations from which the pilot signals stem, that is, locations of the target devices. Furthermore, spatial focusing due to retro-reflection/time-reversal does not suffer from multipath environments [23–27].

The timing sequence of the retro-reflective beamforming scheme is depicted by a flow chart in **Figure 2**. Interactions between the wireless power transmitter and wireless power receiver are toggled among three modes: communication mode, radar mode, and charging mode. The process in **Figure 2** starts when a wireless power receiver (a mobile device, for instance) communicates a "charging request" signal to the wireless power transmitter. Once the wireless power transmitter acknowledges "charging request," the system enters the radar mode in

http://dx.doi.org/10.5772/62855

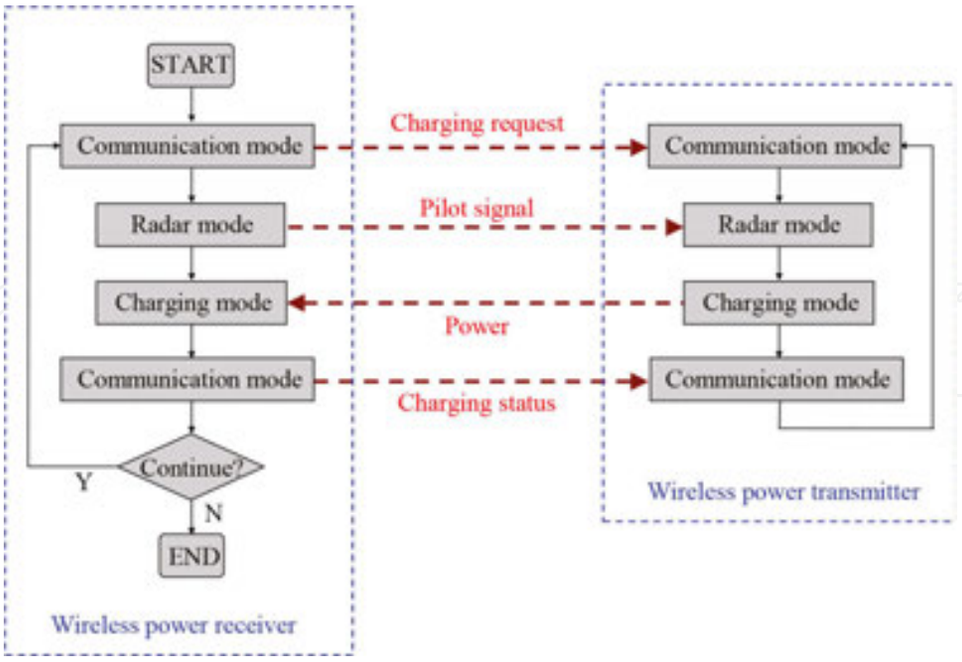

Figure 2. Timing sequence in the retro-reflective beamforming scheme.

which the wireless power receiver transmits pilot signal and the wireless power transmitter prepares for beamforming through analyzing the pilot signal. When the wireless power transmitter is ready, both the wireless power transmitter and wireless power receiver march into the charging mode and power is delivered to the receiver through spatially focused beams. In practice, the environment may change during the charging process; for examples, the wireless power receiver may move and/or another wireless power receiver may request for charging. As a result, the beamforming plan must be adjusted accordingly. To accommodate these situations, the system is periodically switched from the charging mode to the communication mode and the radar mode such that the system would be reconfigured in reaction to the environmental changes.

A system block diagram of the retro-reflective beamforming scheme is plotted in **Figure 3**. The wireless power receiver is assumed to be a mobile/portable device, and thus, it is imperative to minimize its size, weight, and cost. To this end, the wireless power receiver only includes one antenna and two simple circuit blocks. The "pilot signal generator" block in the wireless power receiver is an impulse generator, which generates a periodic train of narrow impulses as the pilot signal. The other block in the wireless power receiver, "microwave-to-DC converter," converts microwave power received from the wireless power transmitter to DC. The wireless power transmitter is composed of multiple antenna elements coordinated by a base station. Behind each antenna element, there are two circuit blocks: a "pilot signal analyzer" and a "microwave power generator." The "pilot signal analyzer" analyzes the pilot signal received from the wireless power receiver, and the "microwave power generator" generates microwave power based on the outcome of analyzing pilot signal. Since the pilot signal is composed of an impulses train, its spectrum covers multiple discrete spectral lines. The

wireless power transmitter selects some of these discrete frequencies to analyze the pilot signal and transmit microwave power. At any discrete frequency, if the pilot signal has phase ϕ, microwave power is generated with phase $-\phi$; in other words, microwave power is configured to be the conjugate version of pilot signal because "phase conjugation in frequency domain" is equivalent to "reversal in time domain" [19].

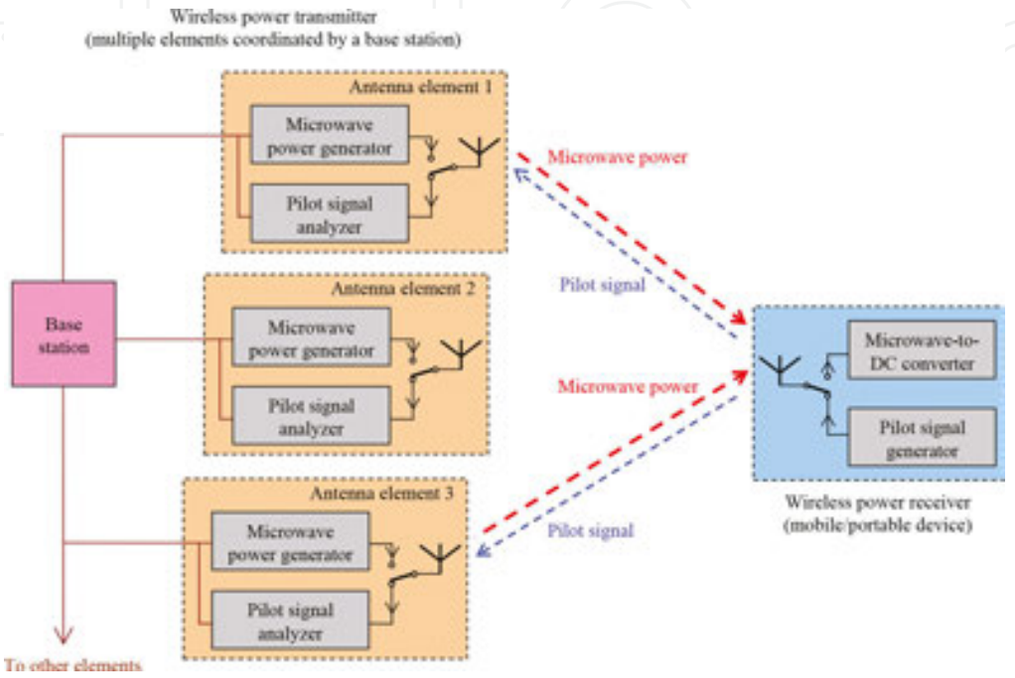

Figure 3. System block diagram of the retro-reflective beamforming scheme [20].

Employing narrow impulses as the pilot signal constitutes one of the major merits of the proposed retro-reflective beamforming scheme. In prior research efforts on retro-reflective beamforming, pilot signals are always generated by a microwave oscillator [28, 29]. Compared with microwave oscillators, impulse generators can be realized using relatively low-complexity and low-power circuitries [30] and hence is more suitable for mobile/portable devices. Because periodic impulses include information over multiple discrete frequencies, the wireless power transmitter has the flexibility of selecting multiple frequencies to transmit microwave power; in contrast, if the pilot signal is a continuous wave, the flexibility is limited to the pilot signal's frequency and its high-order harmonics. Moreover, employing multiple frequencies to carry wireless power would result in better performance in spatial focusing, as demonstrated by some numerical results below.

Figures 4–6 show some numerical results for the retro-reflective beamforming scheme described above. The numerical model is illustrated in **Figure 4**. Eight charging panels are assumed to be deployed over a circular region with radius 3 m in the x–y plane. Each charging panel includes an antenna array with 5 by 5 elements equal spaced by 12 cm. Two devices reside in the region. The antennas over the charging panels and devices are all z-oriented dipoles. The devices transmit short impulses as pilot signals, which cover frequency band [4

http://dx.doi.org/10.5772/62855

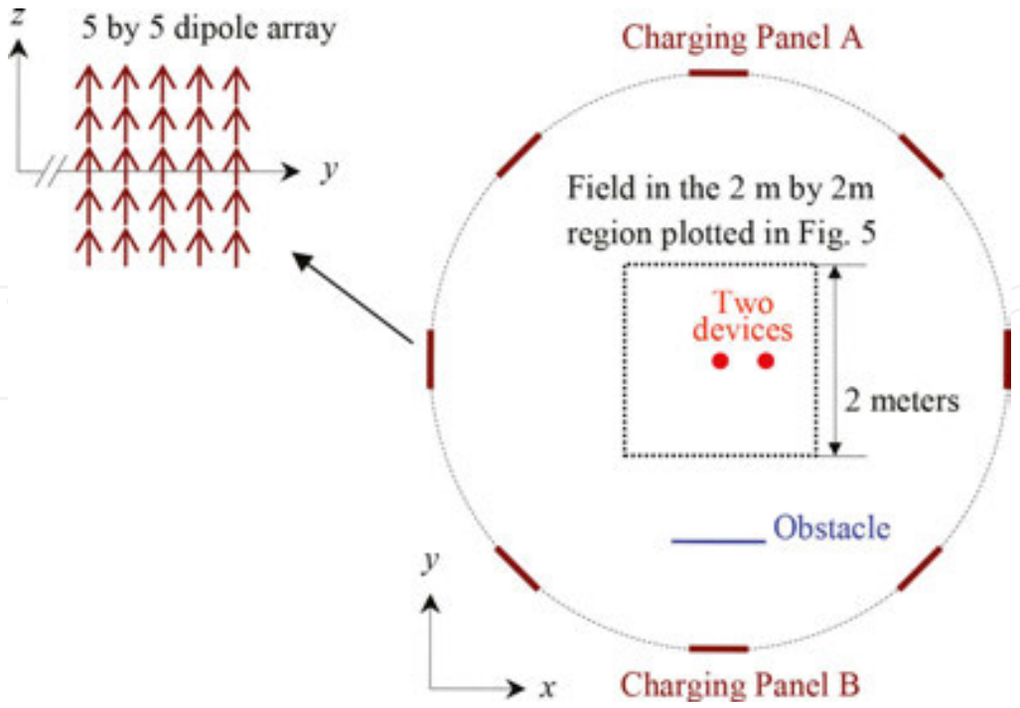

Figure 4. Numerical model of the retro-reflective beamforming scheme [19].

GHz, 6 GHz]. Charging power is allocated to N discrete frequencies in this band. To represent more realistic scenarios, a metallic plate with length 1 m and height 0.6 m is placed to block the line-of-sight path between the devices and one charging panel, which is Charging Panel B in **Figure 4**.

The model in **Figure 4** is simulated by a full-wave solver based on the Method of Moments [19]. Simulated E_z field distributions in a 2 m by 2 m region around the two devices are presented in **Figure 5**. When one device (the one at the center) sends pilot signals to the charging panels with the absence of obstacle, all the eight charging panels are active. If the charging panels only transmit power at one frequency 4.09 GHz (i.e., $N = 1$), the field distribution is shown in **Figure 5(a)**. Apparently, field is focused at many locations other than the device (the undesired focal points resemble side lobes of regular phased beamforming [31]). When N is chosen to be 30, only one focal point remains, which coincides with the device's location, as shown in **Figure 5(b)**. When both devices send pilot signals, the field is automatically focused onto the two devices (**Figure 5(c)**). In **Figure 5(d)**, the obstacle is assumed to be present, and Charging Panel B is blocked and turned off (the other seven charging panels are active). Field focusing does not rely on the obstacle's presence and the number of active charging panels, as shown in **Figure 5(d)**. With the presence of obstacle, which charging panels should be deactivated can be determined through analyzing the pilot signals. Two charging panels, Charging Panel A and Charging Panel B, are used as examples. After these two charging panels receive pilot signals from one device, phase differences between two local antenna elements are plotted in **Figure 6**; one of the two local elements is at the center and the other at the corner in the 5 by 5 array. As expected, since Charging Panel A has line-of-sight interaction with the device, its

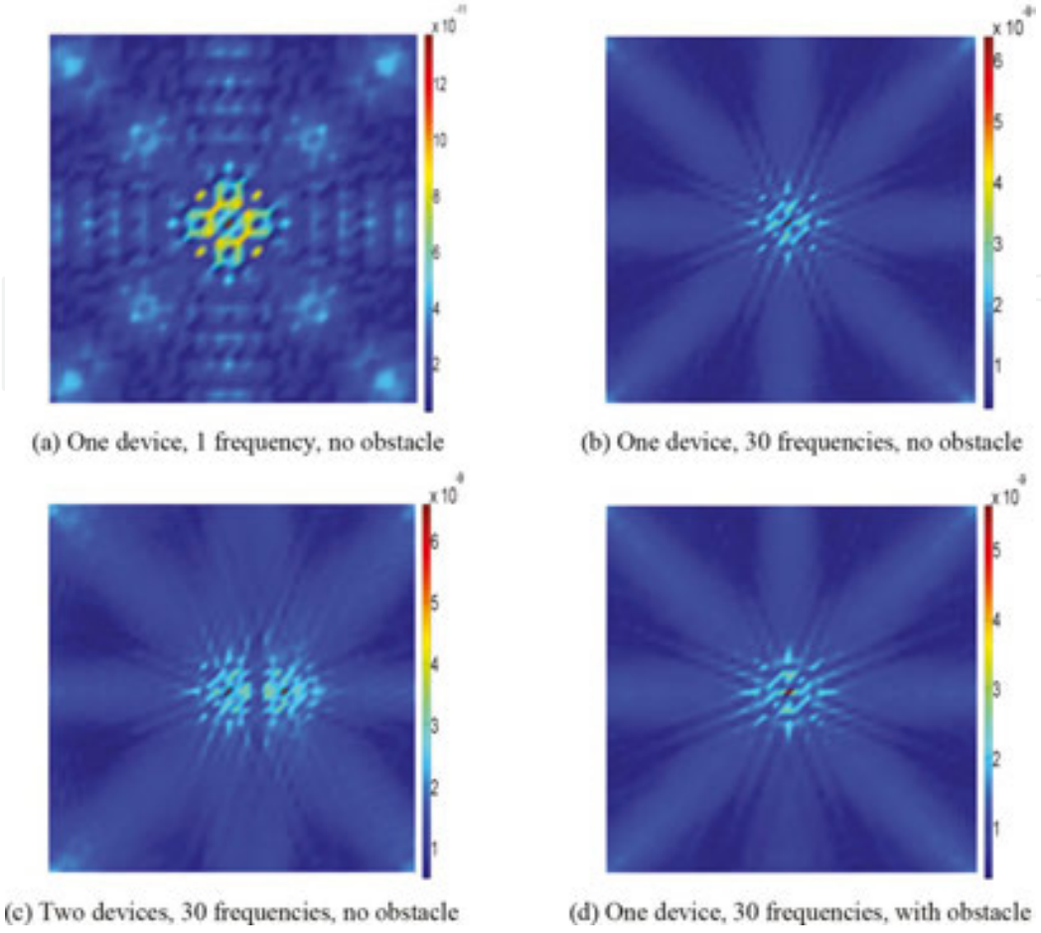

Figure 5. Simulated field distributions of the model in **Figure 4** (with $|E_z|$ represented by colors) [19]. (a) One device, 1 frequency, no obstacle. (b) One device, 30 frequencies, no obstacle. (c) Two devices, 30 frequencies, no obstacle. (d) One device, 30 frequencies, with obstacle

phase difference follows a straight line proportional to the frequency (corresponding to a time delay), whereas such a pattern does not appear at Charging Panel B.

3. Experimental verification of retro-reflective beamforming scheme

We have conducted a range of experimental studies to verify the retro-reflective beamforming scheme described in the previous section [20] [21]. Some of the experimental results are presented in this section.

One of the experimental setup is depicted in **Figure 7**. The wireless power transmitter includes one charging panel, which further includes four microstrip antenna elements. The wireless power receiver has one microstrip antenna. The power transmitter is stationary, whereas the wireless power receiver moves along the x axis in the experiments and it emulates a mobile/portable device. "$x = 0$" denotes the location over the x axis right in front of the charging panel. The distance between "$x = 0$" and the wireless power transmitter is 50 cm.

http://dx.doi.org/10.5772/62855

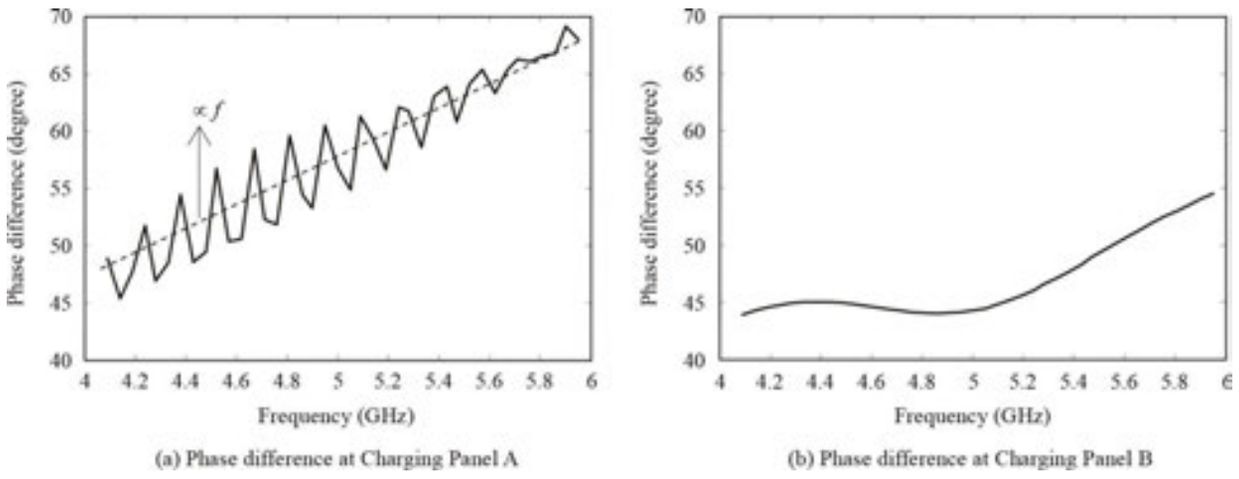

Figure 6. Numerical results of phase difference with the presence of obstacle [19]. (a) Phase difference at Charging Panel A. (b) Phase difference at Charging Panel B.

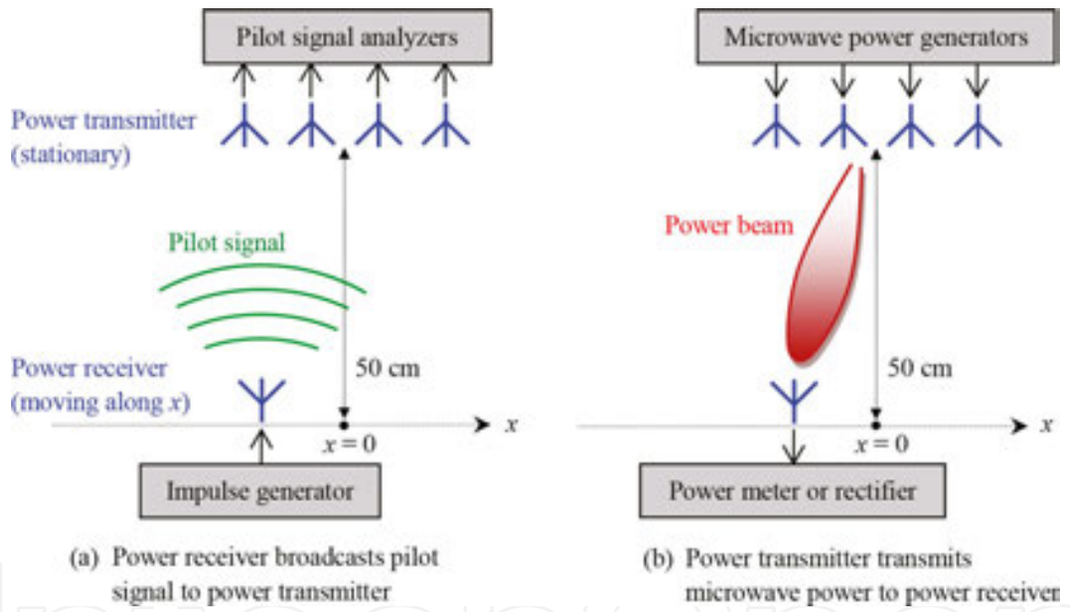

Figure 7. Depiction of an experimental setup with one charging panel [21]. (a) Power receiver broadcasts pilot signal to power transmitter. (b) Power transmitter transmits microwave power to power receiver.

The experimental procedure has the following two steps.

Step (1): Power receiver transmits pilot signal to power transmitter (**Figure 7(a)**). The power receiver's antenna is connected to an impulse generator. The impulses transmitted by the power receiver's antenna behave as the pilot signal. In our implementation, the impulses are generated through amplitude modulating a continuous wave at 2.08 GHz by periodic square impulses with a pulse width of 25 ns and a pulse repetition rate of 4 MHz (its waveform is illustrated in **Figure 8**). The pilot signal is received by the four antennas of the power transmitter and then analyzed by the "pilot signal analyzers."

Step (2): Power transmitter transmits wireless power to power receiver (**Figure 7(b)**). In this step, the power transmitter's four antennas are fed by microwave power generators. The microwave power generators are configured according to the outcome of Step (1) so that a focused power beam is constructed toward the location from which the pilot signal is emitted. Wireless power collected by the power receiver's antenna is detected by either a power meter or a rectifier. The rectifier is implemented by following a voltage multiplier design in [32] and optimized around 2.1 GHz.

A photo of the experimental setup is shown in **Figure 9**: in Step (2), wireless power is delivered from the power transmitter to power receiver and wireless power reception is indicated by a light emitting diode (LED) on the power receiver.

The four antenna elements in the power transmitter are identical to one another. Each is a regular rectangular microstrip patch with dimensions 31.4 mm by 46 mm over FR4 substrate. The four antenna elements are equispaced with the distance between two adjacent elements 7

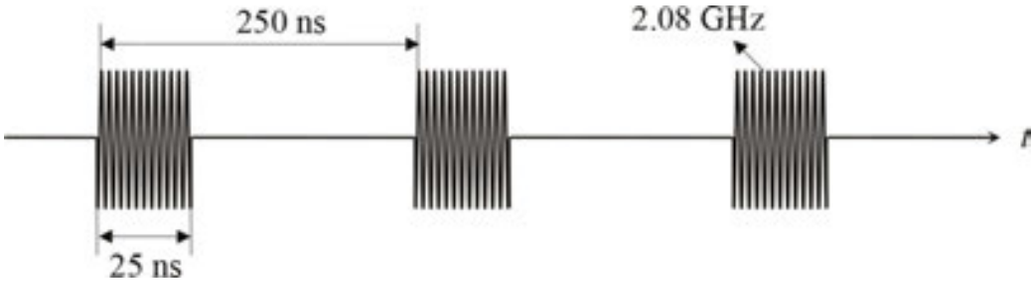

Figure 8. Illustration of the impulse pilot signal.

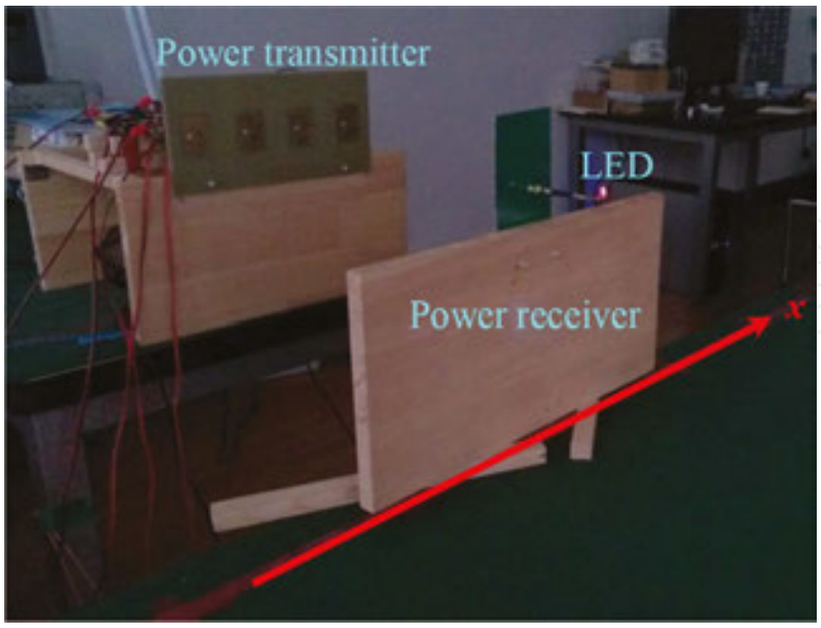

Figure 9. A photo of the experimental setup with one charging panel [21].

cm. Each antenna element's "−10 dB return loss frequency band" is roughly from 2.055 to 2.155 GHz. Each antenna element has a gain value of 3.8 dBi and half-power beamwidth of 136°. The microstrip antenna in the power receiver is the same as those in the power transmitter. All the antennas in **Figure 9** are linearly polarized, and the electric field is polarized along the x direction marked in **Figure 9**.

The two vital blocks in **Figure 7**, "pilot signal analyzers" and "microwave power generators," are illustrated in **Figures 10** and **11**, respectively. In **Figure 10**, the pilot signals received by the four antennas are amplified by four low-noise amplifiers, down-converted through four mixers and a local oscillator at frequency f_{LO}, and then converted to the digital format by a four-channel analog-to-digital converter (ADC). The digital signals are stored within the memory of a personal computer and read by a signal processing program developed in the C++ language. The signal processing program calculates the phases of the four digital signals using short-time (20 μs, to be specific) discrete Fourier transform at the frequency f_{IF}. With the calculated phases (denoted as ϕ_1, ϕ_2, ϕ_3, and ϕ_4), a system control program operates a digital-to-analog converter (DAC), which provides four DC bias voltages (denoted as V_1, V_2, V_3, and V_4) to control the phase shifters in **Figure 11**. The DAC also outputs a control signal V_{CTRL} that is used to turn on/off the oscillator in the microwave power generators. In **Figure 11**, a continuous wave generated by an oscillator at frequency f_t is split into four channels first; next, each channel goes through a phase shifter and power amplification before reaching the antenna. The retro-reflective beamforming is achieved by properly controlling the state of the four phase shifters so that the transmitting array is fed with phases $-\phi_1$, $-\phi_2$, $-\phi_3$, and $-\phi_4$, respectively. This is done by the system control program that determines the output DC bias voltages of the DAC based on the characteristics of the four phase shifters. The system control program is also responsible for controlling the operation sequence of the entire system. Specifically, in Step (1) of the experiment, the system control program activates the ADC and calls the signal processing program to analyze the pilot signal. In the meantime, the oscillator in the microwave power generators is turned off by the control signal V_{CTRL} to avoid the interference of microwave power to the pilot signal analyzers. In Step (2), the system control program deactivates the ADC and reset V_{CTRL} to turn on the oscillator so that the wireless power is transmitted.

The pilot signal analyzers and microwave power generators are implemented using commercial off-the-shelf components with model numbers listed in **Figures 10** and **11**. The mixers, amplifiers, and the oscillators are made by Analog Devices Inc. The four phase shifters are made by Beijing Tianhua Zhongwei Technology. The 1:4 power splitters are made by Mini-Circuits. The ADC and DAC are made by Beijing Art Technology Development Co. The ADC PCI8502 provides four synchronized channels with a sampling rate of 40 MHz and 12-bit resolution. The DAC PCI8250 provides eight synchronized channels with 16-bit resolution.

Employing impulses as the pilot signal leads to the flexibility of configuring f_t. The pilot signal's spectrum is centered at 2.08 GHz and contains discrete spectral lines with separation of 4 MHz. In one of the implementations, f_t = 2.08 GHz with f_{LO} = 2.079 GHz and f_{IF} = 1 MHz. f_t can be reconfigured to other frequencies straightforwardly; for instance in another implementation, f_t is reconfigured to be 2.108 GHz with f_{LO} = 2.1 GHz and f_{IF} = 8 MHz.

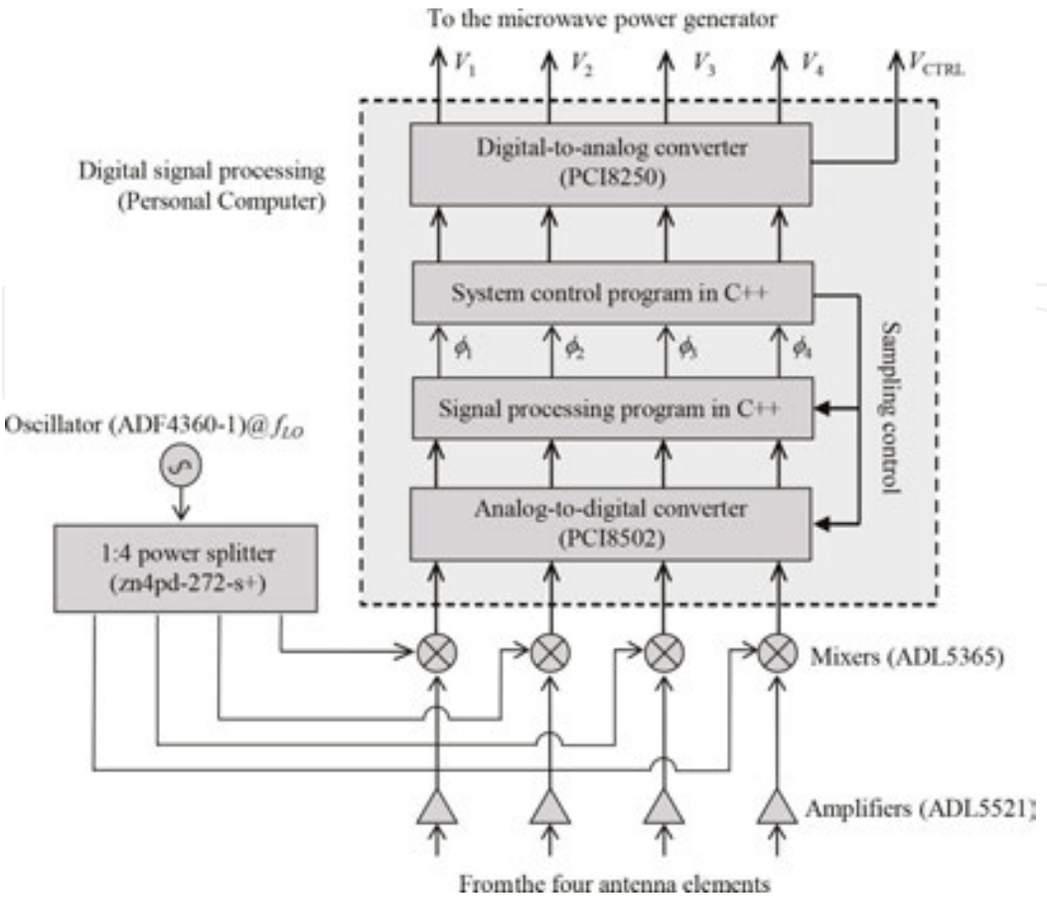

Figure 10. Block diagram of "pilot signal analyzers."

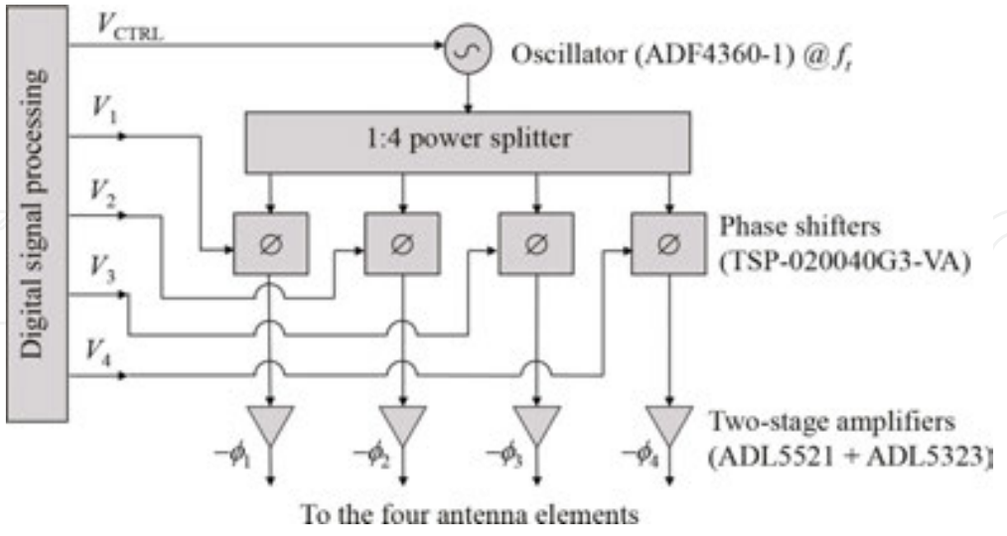

Figure 11. Block diagram of "microwave power generators."

http://dx.doi.org/10.5772/62855

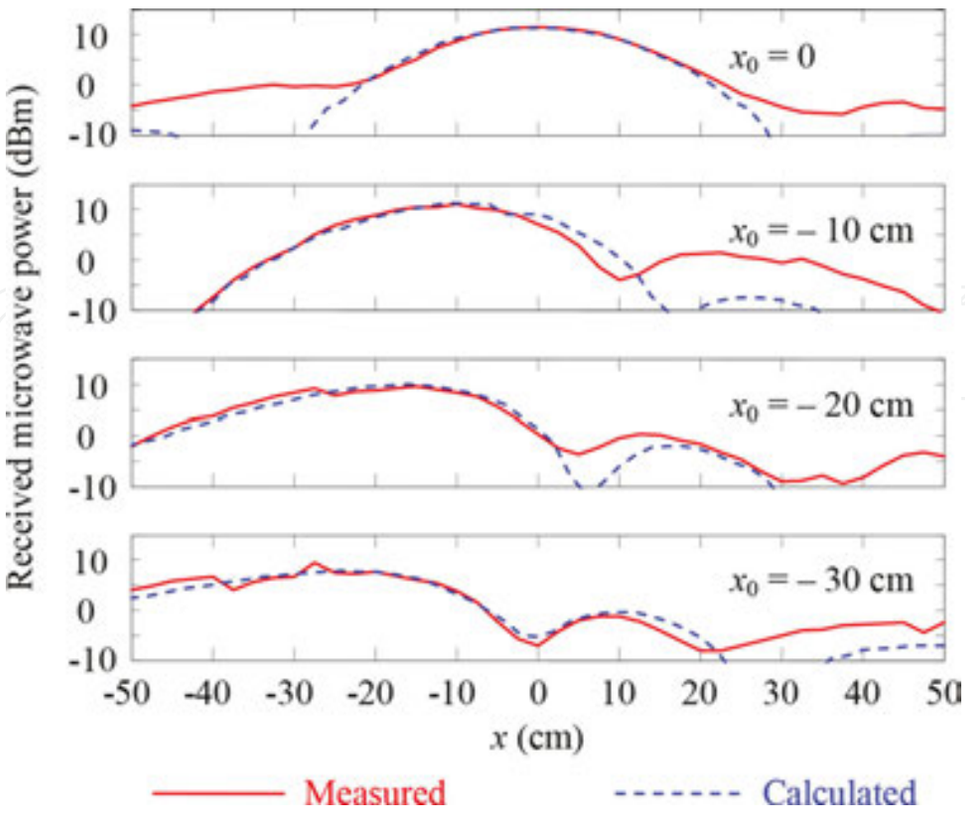

Figure 12. Received microwave power at frequency 2.08GHz [21].

In the experiments, a pilot signal is broadcasted by the power receiver at a location denoted as x_0, and the pilot signal is received and analyzed by the power transmitter; then after the power transmitter is configured by the outcome of analyzing the pilot signal, the power receiver moves along x axis to detect the wireless power. In all the experiments, the total power transmitted by the power transmitter is roughly 1 Watt (that is, 250 mW from each of its four antennas).

In **Figure 12**, microwave power measured by a power meter is plotted when $f_t = 2.08$ GHz. The four subplots in **Figure 12** correspond to "$x_0 = 0$," "$x_0 = -10$ cm," "$x_0 = -20$ cm," and "$x_0 = -30$ cm," respectively. The calculated curves in **Figure 12** are obtained using the Friis transmission equation [31]

$$P_r = P_t\left(\frac{\lambda}{4\pi d}\right)^2 G_t G_r$$

When $x_0 = 0$ and $x = 0$, the transmitted power $P_t = 1$ Watt, wavelength $\lambda = c/f_t$, c is the speed of light in free space, the transmitter–receiver distance $d = 50$ cm, the transmitting antenna's gain $G_t = 9.8$ dBi, the receiving antenna's gain $G_r = 3.8$ dBi, and the received power P_r is calculated to be 12 mW. In **Figure 12**, the measured data and calculated data generally match each other.

The measured data in reaction to "$x_0 = 0$" have a peak at "$x = 0$," with peak value of the received power about 14 mW. The measured value (14 mW) is slightly larger than the calculated value (12 mW); we believe it is because the power receiver does not reside in the power transmitter's far-zone, which makes Friis equation not very precise. When x_0 changes to −10, −20, and −30 cm, the power beam is steered and the beam center tracks x_0. In our experiments, the beam cannot be steered beyond −30 cm due to the limitation of individual microstrip antennas' radiation patterns. When x_0 takes positive values, the power beam is steered and the beam center tracks x_0 as well; beam steering for positive x_0 values is not demonstrated because it is symmetric to the negative x_0 values. Similar sets of results are displayed in **Figure 13**, after the power meter is replaced by the rectifier. The vertical axis in **Figure 13** represents the DC voltage measured over a 1.8-kΩ load resistor in the rectifier. Beams in reaction to four x_0 values are clearly shown. When $x_0 = 0$, the peak voltage 3.5 V corresponds to $(3.5)^2/(1.8\text{ k}) \cong 7$ mW.

After f_t is reconfigured to 2.108 GHz, curves similar to those in **Figure 12** are plotted in **Figure 14**. The beamforming phenomena exhibited in **Figure 14** are basically the same as those in **Figure 12**.

On the basis of the experimental setup in **Figure 7**, another set of experiments are carried out as illustrated in **Figure 15**. As a progress with respect to **Figure 7**, the wireless power transmitter in **Figure 15** includes two charging panels, each consisting of four antenna elements. The two charging panels are placed over x axis and y axis, respectively. The wireless power receiver moves within a certain region in the x–y plane. **Figure 16** shows a photo of the

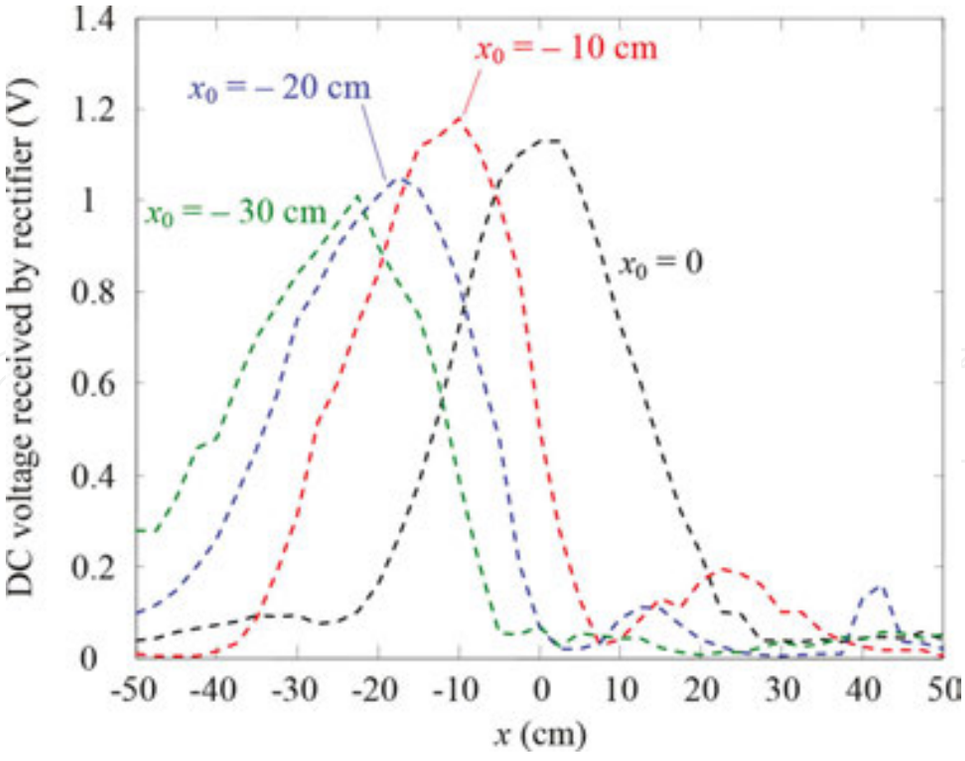

Figure 13. Received DC voltage at frequency 2.08GHz [21].

http://dx.doi.org/10.5772/62855

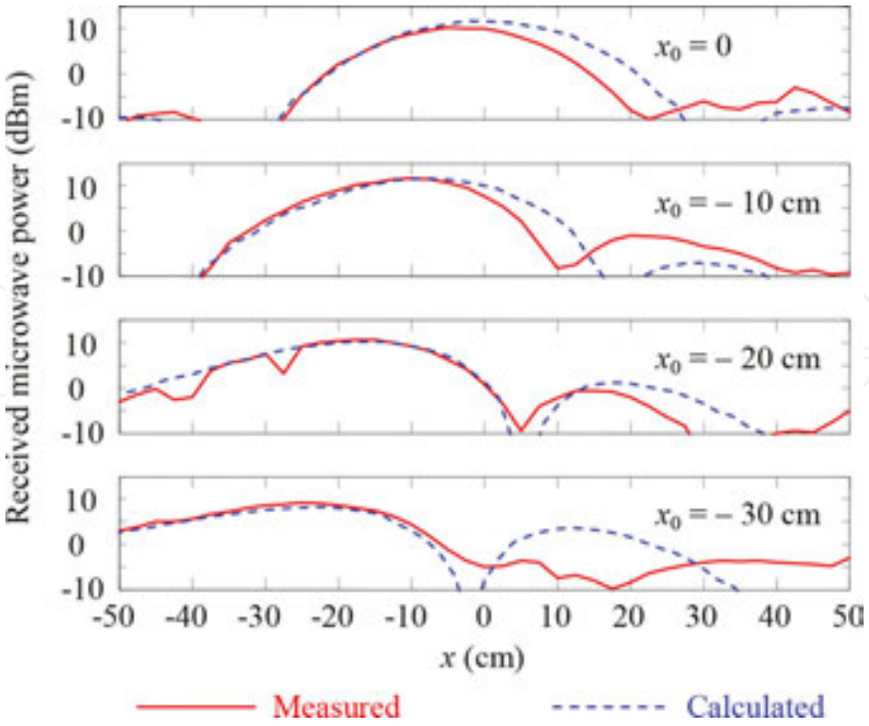

Figure 14. Received microwave power at frequency 2.108 GHz [21].

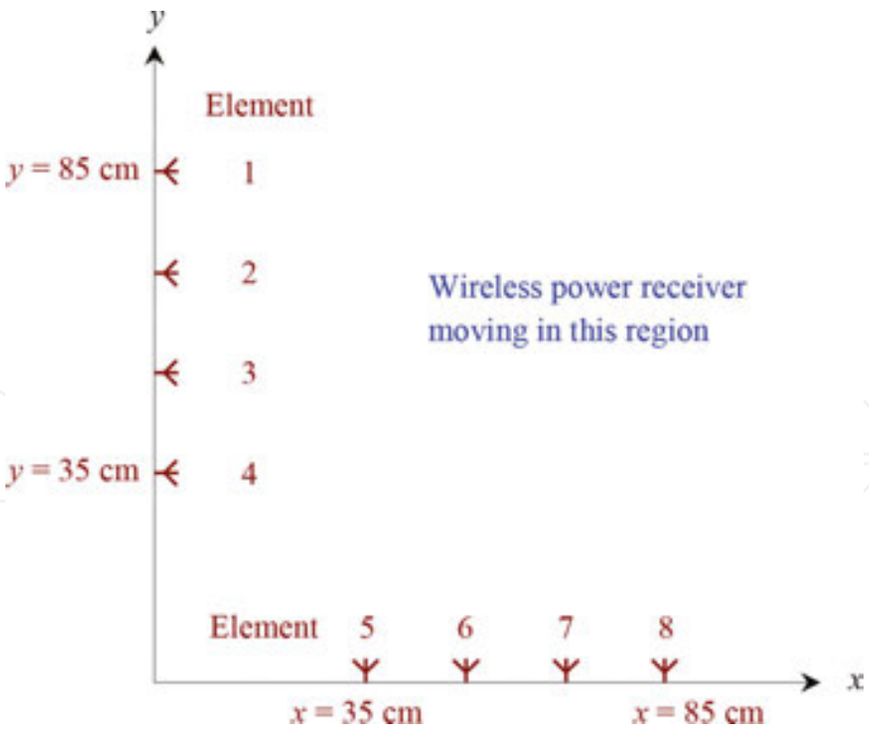

Figure 15. Illustration of an experimental setup with two charging panels [20].

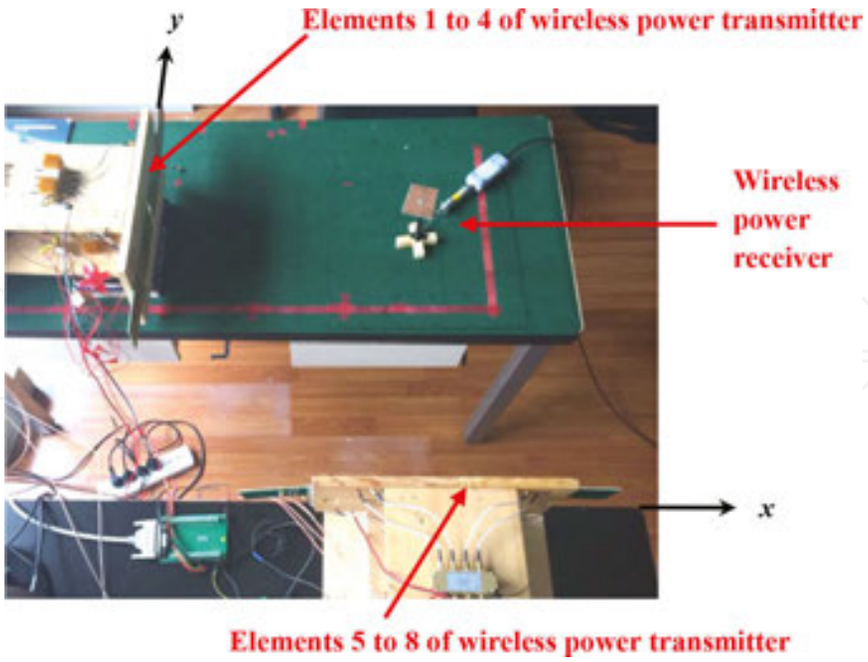

Figure 16. A photo of the experimental setup with two charging panels [20].

experimental setup corresponding to **Figure 15**. The antennas of the wireless power transmitter are microstrip antennas polarized along z direction; the antenna of the receiver is a monopole antenna, with omni-directional radiation pattern in the x–y plane.

Some results measured with the configuration in **Figures 15** and **16** are shown in **Figure 17**. The microwave power transmitted by each antenna element of the wireless power transmitter is roughly 175 mW, with a total of 175 mW × 8 = 1.4 Watt. A power meter is connected to the wireless power receiver's antenna, and the measured microwave power is plotted in **Figure 17**. The two plots in **Figure 17(a)** and **(b)** are obtained when the pilot signal is broadcasted from (x = 60 cm, y = 60 cm) and (x = 70 cm, y = 70 cm), respectively. **Figure 17** clearly demonstrates that the microwave power is focused onto the location from which the pilot signal is broadcasted as a result of retro-reflective beamforming.

4. Conclusion

This chapter presents a retro-reflective beamforming scheme aiming to supply microwave power to portable/mobile electronic devices over long distances (several meters or longer) efficiently. The preliminary numerical and experimental results demonstrate that the proposed retro-reflective beamforming scheme is capable of focusing microwave power onto target devices' locations through analyzing pilot signals broadcasted by the target devices. We are currently conducting research to verify the retro-reflective beamforming scheme more comprehensively.

http://dx.doi.org/10.5772/62855

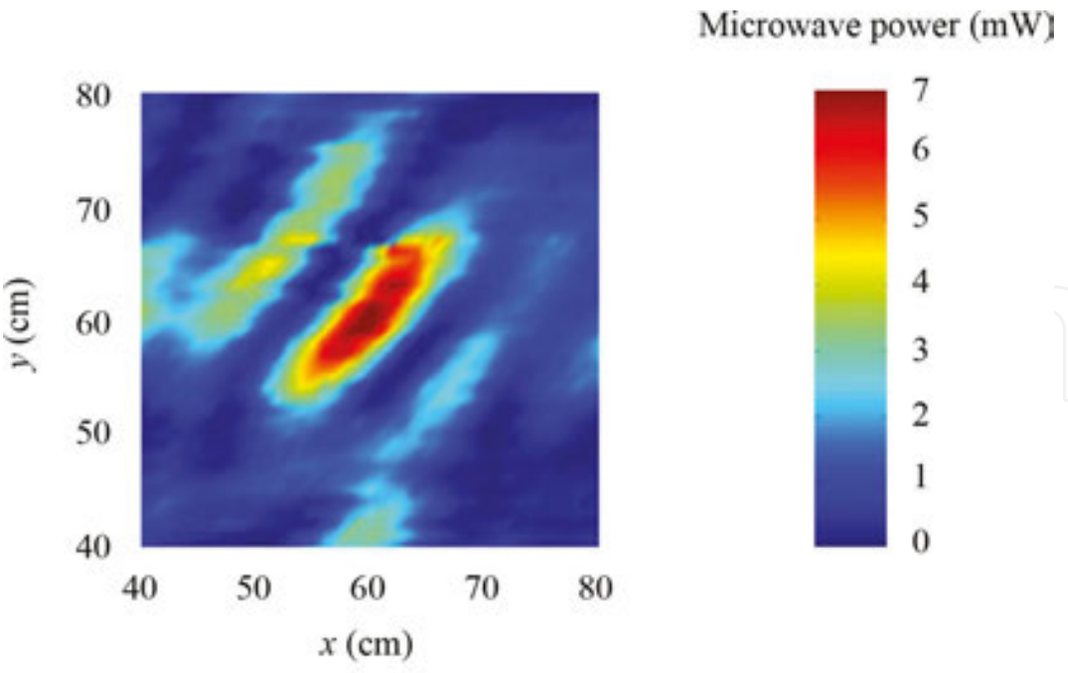

(a) Pilot signal from (x = 60 cm, y = 60 cm)

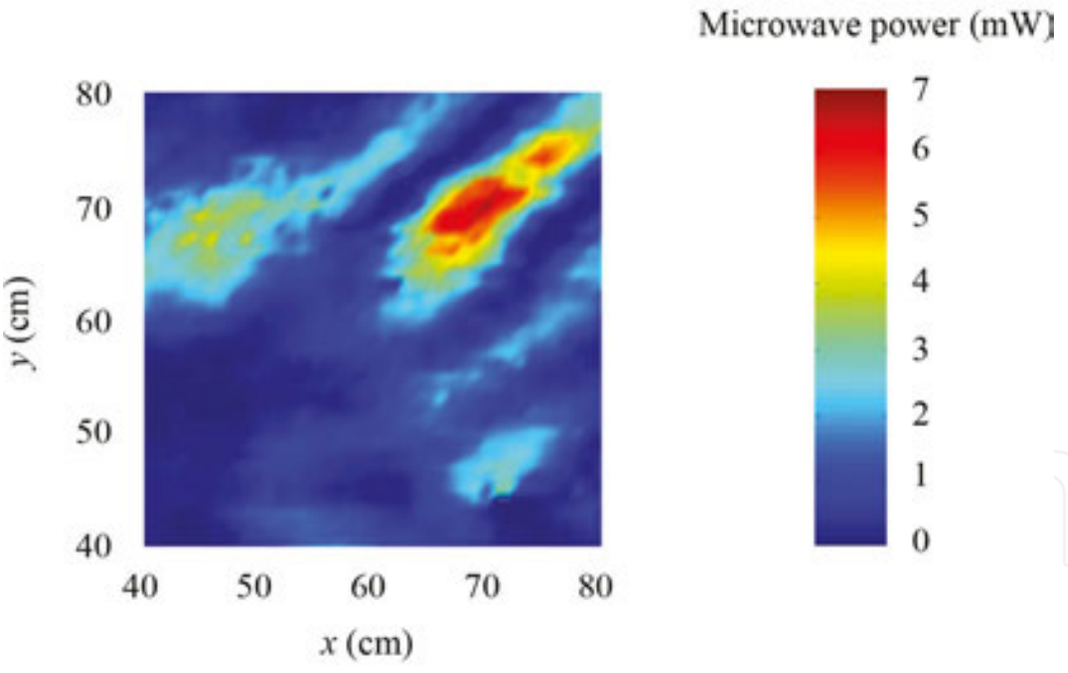

(b) Pilot signal from (x = 70 cm, y = 70 cm)

Figure 17. Microwave power distribution measured with the configuration in **Figures 15** and **16** [20]. (a) Pilot signal from (x = 60 cm, y = 60 cm). (b) Pilot signal from (x = 70 cm, y = 70 cm).

Acknowledgements

This work was supported in part by National Science Foundation Grant ECCS 1303142, National Science Foundation Grant ECCS 1503600, and National Natural Science Foundation of China Grant 61471195

Author details

Xin Wang[1*] and Mingyu Lu[2*]

*Address all correspondence to: wang90@nuaa.edu.cn and mingyu.lu@mail.wvu.edu

1 College of Electronic and Information Engineering, Nanjing University of Aeronautics and Astronautics, Nanjing, China

2 Department of Electrical and Computer Engineering, West Virginia University Institute of Technology, Montgomery, WV, USA

References

[1] Brown WC. The history of power transmission by radio waves. Microwave Theory and Techniques, IEEE Transactions on. 1984;32(9):1230–42.

[2] Lee TH. Planar microwave engineering: A practical guide to theory, measurement, and circuits. Cambridge University Press; Cambridge, UK; New York, 2004.

[3] Strassner B, Chang K. Microwave power transmission: Historical milestones and system components. Proceedings of the IEEE. 2013; 101(6):1379–96.

[4] Garnica J, Chinga RA, Lin J. Wireless power transmission: From far field to near field. Proceedings of the IEEE. 2013; 101(6):1321–31.

[5] Kim SM, Kim SM. Wireless optical energy transmission using optical beamforming. Optical Engineering. 2013; 52(4):043205.

[6] Brown WC. Experimental airborne microwave supported platform. Spencer Lab Report, Raytheon CO: Burlington MA; 1965.

[7] Dickinson RM. Safety issues in SPS wireless power transmission. Space Policy. 2000;16(2):117–22.

[8] Lan Sun Luk JD, Celeste A, Romanacce P, ChaneKuang Sang L, Gatina JC. Point-to-point wireless power transportation in Reunion Island. In 48th International Astronautical Congress, Turin, Italy, October 1997.

[9] Celeste A, Jeanty P, Pignolet G. Case study in Reunion Island. Acta Astronautica. 2004;54(4):253–8.

[10] Zhao X, Qian T, Popovic Z, Zane R, Mei G. Wireless ultrasonic transducer network for structural health monitoring of an aircraft wing. In 17th World Conference on Non-destructive Testing. Shanghai, China, October 2008, pp. 1–8.

[11] Mascarenas DL, Flynn EB, Todd MD, Overly TG, Farinholt KM, Park G, Farrar CR. Experimental studies of using wireless energy transmission for powering embedded sensor nodes. Journal of Sound and Vibration. 2010;329(12):2421–33.

[12] Visser HJ, Vullers RJM. RF energy harvesting and transport for wireless sensor network applications: Principles and requirements. Proceedings of the IEEE. 2013; 101(6):1410–23.

[13] McSpadden JO, Fan L, Chang K. Design and experiments of a high-conversion-efficiency 5.8-GHz rectenna. Microwave Theory and Techniques, IEEE Transactions on. 1998;46(12):2053–60.

[14] Ren YJ, Chang K. 5.8-GHz circularly polarized dual-diode rectenna and rectenna array for microwave power transmission. Microwave Theory and Techniques, IEEE Transactions on. 2006;54(4):1495–502.

[15] Landis GA, inventor; Nasa Glenn Research Center, Assignee. Charging of devices by microwave power beaming. United States patent US 6,967,462. 2005.

[16] IEEE C95.1-2005: IEEE standard for safety levels with respect to human exposure to radio frequency electromagnetic fields, 3 kHz to 300 GHz. IEEE. 2006.

[17] Rules & Regulations for Title 47, Federal Communications Commission. https://www.fcc.gov/general/rules-regulations-title-47.

[18] ICNIRP (International Commission for Non-Ionizing Radiation Protection) Standing Committee on Epidemiology. Epidemiology of health effects of radiofrequency exposure. Environmental Health Perspectives. 2004;112(17):1741–54.

[19] Zhai H, Pan HK, Lu M. A practical wireless charging system based on ultra-wideband retro-reflective beamforming. In Antennas and Propagation Society International Symposium, IEEE. Toronto, Ontario, July 2010.

[20] He J, Wang X, Guo L, Shen S, Lu M. A distributed retro-reflective beamformer for wireless power transmission. Microwave and Optical Technology Letters. 2015;57(8): 1873–6.

[21] Wang X, Sha S, He J, Guo L, Lu M. Wireless power delivery to low-power mobile devices based on retro-reflective beamforming. Antennas and Wireless Propagation Letters, IEEE. 2014;13:919–22.

[22] Henty BE, Stancil DD. Multipath-enabled super-resolution for RF and microwave communication using phase-conjugate arrays. Physical Review Letters. 2004;93(24): 243904.

[23] Fink M. Time reversal of ultrasonic fields. I. Basic principles. Ultrasonics, Ferroelectrics, and Frequency Control, IEEE Transactions on. 1992;39(5):555–66.

[24] Wu F, Thomas JL, Fink M. Time reversal of ultrasonic fields. II. Experimental results. Ultrasonics, Ferroelectrics, and Frequency Control, IEEE Transactions on. 1992;39(5): 567–78.

[25] Fannjiang A, Solna K. Superresolution and duality for time-reversal of waves in random media. Physics Letters A. 2005;342(1):22–9.

[26] Lerosey G, De Rosny J, Tourin A, Fink M. Focusing beyond the diffraction limit with far-field time reversal. Science. 2007;315(5815):1120–2.

[27] De Rosny J, Fink M. Focusing properties of near-field time reversal. Physical Review A. 2007;76(6):065801.

[28] Chang Y, Fetterman HR, Newberg IL, Panaretos SK. Microwave phase conjugation using antenna arrays. Microwave Theory and Techniques, IEEE Transactions on. 1998;46(11):1910–9.

[29] Chiu L, Yum TY, Chang WS, Xue Q, Chan CH. Retrodirective array for RFID and microwave tracking beacon applications. Microwave and Optical Technology Letters. 2006;48(2):409–11.

[30] Fontana R, Ameti A, Richley E, Beard L, Guy D. Recent advances in ultra wideband communications systems. In IEEE Conference on Ultra Wideband Systems and Technologies. Baltimore, Maryland, May 2002, pp. 129–133.

[31] Balanis CA. Antenna theory: analysis and design. John Wiley & Sons; Hoboken, New Jersey, 2005.

[32] Lamantia A, Maranesi PG, Radrizzani L. Small-signal model of the Cockcroft-Walton voltage multiplier. Power Electronics, IEEE Transactions on. 1994;9(1):18–25.